Articles

Contribution from the Department of Inorganic Chemistry,
University of Umeå, S-901 87 Umeå, Sweden

Equilibrium and Structural Studies of Silicon(IV) and Aluminum(III) in Aqueous Solution. 17. Stable and Metastable Complexes in the System H^+–Al^{3+}–Citric Acid[†]

Lars-Olof Öhman

Received February 3, 1988

The kinetic route for complexation of citric acid (H_3Cit) to Al^{3+} was studied by time-dependent potentiometric measurements in the range $3 < -\log [H^+] < 7$. It is shown that two mononuclear species, $Al(H_{-1}Cit)^-$ and $Al(OH)(H_{-1}Cit)^{2-}$, determine the speciation in freshly prepared solutions. As the solutions age, these are converted into the thermodynamically more stable species $Al_3(OH)(H_{-1}Cit)_3^{4-}$. In the paper, distribution diagrams showing this conversion as a function of time and $-\log [H^+]$ are presented. In slightly alkaline solutions, $7 < -\log [H^+] < 9.5$, the appearance of another slow-forming mixed trinuclear species, $Al_3(OH)_4(H_{-1}Cit)_3^{7-}$, is demonstrated. Experimental data indicate that the two trinuclear species are *not* structurally interrelated. All measurements were performed in 0.6 M NaCl medium at 25 °C, and data were analyzed by using the least-squares computer program LETAGROPVRID. To indicate the complexing ability of citrate ions to Al(III) in natural waters, the solubility of aluminum hydroxide (gibbsite and highly amorphous $Al(OH)_3$) was calculated as a function of citrate concentration and pH. Through these calculations, the importance of mononuclear complexes at low citrate concentrations is emphasized. Under typical blood plasma conditions (10^{-6} M Al(III); 10^{-4} M Cit), the existence of polynuclear species is negligible. The dominating species at pH ~7.4 is $Al(OH)(H_{-1}Cit)^{2-}$.

Introduction

During the last 15 years, it has been firmly established that different aqueous aluminum species exhibit severe toxic effects to man[1] as well as to plants,[2] fish,[3] and other forms of aquatic life.[4] It has also been established that the uptake and toxicity is correlated to certain aqueous complexes rather than to total concentrations.[5–7] For that reason, the interest in the aqueous coordination chemistry of Al^{3+} with naturally occurring ligands has considerably increased during recent years.

Concerning the title ligand, citric acid (H_3Cit), which is one of the preeminent low-molecular-weight metal binders in blood plasma as well as a most abundantly occurring substance in nature, no less than six articles[8–11] or abstracts[12,13] have appeared during the last few years. Unfortunately, however, the complexation models presented in the different articles are quite contradictory. Only with regard to the most acidic species, $AlHCit^+$ and $AlCit^0$, which appear in solutions with pH values below ~3, do the different investigations agree.

The main reason for the divergence obtained in less acidic solutions seem to be the fact that equilibration in such solutions is extremely sluggish. Thus, while we[9] found that equilibration times up to 6 h between base additions were necessary, others[8,11] have stated that much shorter time intervals were used. This probably means that published complexation models represent mixtures between equilibrium and nonequilibrium complexes.

Furthermore, Gregor et al.[11] have tried to evaluate an equilibrium model solely from high ligand/metal ratio data where the dominating measurable quantity actually is a neutralization of unbound citric acid. Under such experimental conditions, it can easily be shown that unless data have been collected with extreme precision, almost any model can be used to explain experimental data.

The purpose of the present paper is to investigate the complexation route of citric acid to Al^{3+}, from the time of mixing to the time where true equilibrium has been established in the system. We also investigate the complexation features of citrate ions to Al^{3+} in slightly alkaline solutions, an area not covered in our earlier contribution.[9]

Experimental Section

Chemicals and Analysis. The preparation and analysis of citric acid solutions is described in ref 9 while the preparation of other solutions is described in ref 14.

Apparatus. The automatic system for precise emf titrations, the thermostat, and the cell arrangement are fully described elsewhere.[14] The calibration of the glass electrode was performed separately in solutions of known $[H^+]$ before and after each experiment. In order to protect neutral and slightly alkaline aluminum–citrate solutions from uptake of atmospheric carbon dioxide, these solutions were stored under argon and purged with argon gas during $-\log [H^+]$ measurements. The turbidimetric measurements were performed with a Hach Model 18900 ratio turbidimeter.

Temperature and Medium. The present investigation was carried out at 25.00 ± 0.05 °C in a constant ionic medium of 0.6 M Na(Cl).

Method. As mentioned in the Introduction, the aim of this investigation is 2-fold. One aim is to determine the kinetic route to true equilibrium in slightly acidic ($-\log [H^+] \approx 3$–7) aluminum–citrate solutions, and the other aim is to determine equilibrium speciation in neutral and slightly alkaline solutions.

To meet the first aim, it is necessary to use an experimental approach that makes it possible to follow the formation of both fast- and slow-

---

[†] Presented in a session lecture at the symposium "Environmental Chemistry of Aluminum", 194th National Meeting of the American Chemical Society, Division of Environmental Chemistry, New Orleans, LA, Aug 1987.

(1) Ganrot, P. O. *EHP, Environ. Health Perspect.* **1986**, *65*, 363–441 and references therein.

(2) Ulrich, B.; Mayer, R.; Khanner, P. K. *Schriften aus der forstlichen Fakultät der Universität Göttingen und der Niedersäcksischen forstlichen Versuchsanstalt*; J. D. Sauerländers: Frankfurt am Main, FRG, 1979; Vol. 58, 1979.

(3) Rosseland, B. O.; Skogheim, O. K. *ICES, C.M.* **1982**, *M29*, 1–15 (Proceedings from a conference held in Bergen, Norway, June 1982: Symposium on Fisheries Acoustics; International Council for the Exploration of the Sea).

(4) Clark, K.; LaZerte, B. *Can. J. Fish. Aquat. Sci.* **1985**, *42*, 1544–1551.

(5) Slanina, P.; Falkeborn, Y.; Frech, W.; Cedergren, A. *Food Chem. Toxicol.* **1984**, *22*, 391–397.

(6) Parker, D. R.; Zelazny, L. W.; Kinraide, T. B. *Prepr. Pop., Nat. Meet.—Am. Chem. Soc., Div. Environ. Chem.* **1987**, *27*(2), 369–372.

(7) Baker, J. P.; Schofield, C. L. *Water, Air, Soil Pollut.* **1982**, *18*, 289–310.

(8) Jackson, G. E. *S. Afr. J. Chem.* **1982**, *35*(3), 89–92.

(9) Öhman, L.-O.; Sjöberg, S. *J. Chem. Soc., Dalton Trans.* **1983**, 2513–2517.

(10) Motekaitis, R. J.; Martell, A. E. *Inorg. Chem.* **1984**, *23*, 18–23.

(11) Gregor, J. E.; Powell, H. K. J. *Aust. J. Chem.* **1986**, *39*, 1851–1864.

(12) Findlow, J. A.; Duffield, J. R.; Evans, D. A.; Williams, D. R. *Recl. Trav. Chim. Pays-Bas* **1987**, *106*, 403.

(13) Vanturini, M.; Berthon, G.; May, P. M. *Recl. Trav. Chim. Pays-Bas* **1987**, *106*, 406.

(14) Öhman, L.-O.; Sjöberg, S. *Acta Chem. Scand., Ser A* **1981**, *A35*, 201–212.

0020-1669/88/1327-2565$01.50/0

Table I. Previously Determined Binary and Ternary Complexes in the Three-Component System H^+–Al^{3+}–Citric Acid[a]

(p,q,r)	tentative struct	$\log \beta_{p,q,r}$	ref
(–1,0,1)	H_2Cit^-	–2.769	9
(–2,0,1)	$HCit^{2-}$	–6.850	9
(–3,0,1)	Cit^{3-}	–12.067	9
(–1,1,0)	$Al(OH)^{2+}$	–5.52	15
(–2,1,0)	$Al(OH)_2^+$	–11.3	17, 18
(–3,1,0)	$Al(OH)_3^0$	–17.3	17, 18
(–4,1,0)	$Al(OH)_4^-$	–23.46	16
(–4,3,0)	$Al_3(OH)_4^{5+}$	–13.57	15
(–32,13,0)	$Al_{13}O_4(OH)_{24}^{7+}$	–109.2	15
(–2,1,1)	$AlHCit^+$	–2.68	9
(–3,1,1)	$AlCit^0$	–4.92	9
(–6,1,2)	$Al(Cit)_2^{3-}$	–12.53	9
(–13,3,3)	$Al_3(OH)(H_{-1}Cit)_3^{4-}$	–21.77	9

[a] The formation constants are related to the reaction $pH^+ + qAl^{3+} + rH_3Cit \rightleftharpoons H_pAl_q(H_3Cit)_r^{p+3q}$.

forming complexes. The approach used in this work can be described as follows: To an acidic aluminum–citrate solution containing only the species Al^{3+}, $AlHCit^+$, and $AlCit^0$ (–log $[H^+] \approx 2$), in which the glass electrode had been equilibrated, hydroxide ions were quickly added in one sudden portion under intense stirring of the solution to a predetermined H level (H is the total proton concentration with H_2O, Al^{3+}, H_3Cit as zero level). Resulting –log $[H^+]$ values were thereafter recorded as a function of time until true equilibrium (i.e. stable emf potentials remaining constant to 0.02 mV for several hours) had been attained in the system (>12 h). For every new H level investigated, the procedure was repeated from a new acidic aluminum–citrate solution.

To meet the second aim, it is necessary to collect equilibrium data with as large a variation in total aluminum concentration, B, total citric acid concentration, C, and –log $[H^+]$ as possible. As it turned out that the equilibration also in this region was very sluggish, with equilibration times of up to 20 h, these data were collected from batch solutions that had been equilibrated under an argon atmosphere for 1 week. To ensure that no solid aluminum hydroxide had formed in these solutions, also turbidimetric measurements were undertaken. In the evaluation of the equilibrium model, only data from clear solutions were used.

Data Treatment. The equilibria under consideration in the present study can be divided into three groups as follows: (1) ionization of citric acid, (2) hydrolysis of Al^{3+}, and (3) general formation of three-component equilibria. In earlier parts of this series,[9,15,16] formation constants for dominating binary as well as for mono- and polynuclear ternary complexes have been determined. These constants are given in Table I. In addition, the table also contains recalculated values for the formation constants of $Al(OH)_2^+$ and $Al(OH)_3^0$ in 0.6 M NaCl solution. In this recalculation, equations given by Baes and Mesmer[17] together with β^0 values given by Dyrssen[18] were used.

In the evaluation of kinetic effects in freshly prepared acidic solutions all of these equilibrium constants, except the one for (–13,3,3), which was put to zero, will be considered as known and no attempts will be made to vary them. For neutral and slightly alkaline equilibrium data, data in Table I, together with findings made in slightly acidic solutions, are the base from which the equilibrium analysis is built.

Computer Programs. Calculations of theoretical titration curves from published complexation models and the distribution of polynuclear species as a function of stability constants as well as the calculation and plotting of distribution, solubility, and predominance area diagrams were all performed with the program SOLGASWATER.[19] The evaluation of experimental data was performed with the least-squares program LETAGROPVRID,[20] version ETITR.[21,22] In these computations, the error squares sum $U = \sum(H_{calcd} - H_{exptl})^2$ was minimized. The standard deviations reported are defined according to Sillén.[23,24] The computations were all performed on a CD Cyber 850 computer.

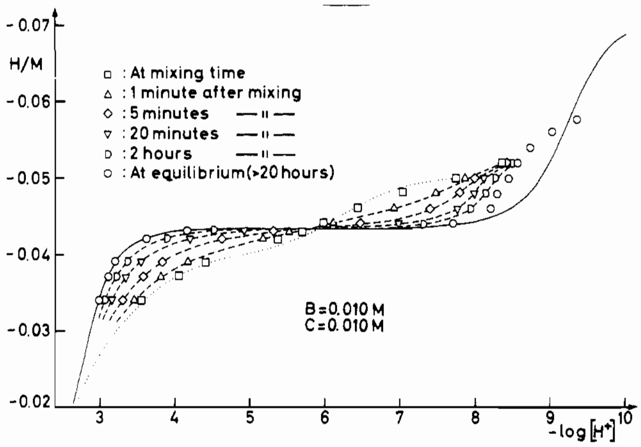

Figure 1. Part of the experimental data, $B = C$ 0.010 M, plotted as curves of H versus –log $[H^+]$ at different times after solution preparation. The solid curve was calculated by using the set of constants in Table I. The dotted curve was generated through an exchange of $(-13,3,3)^{4-}$ for $(-4,1,1)^-$ and $(-5,1,1)^{2-}$ with the equilibrium constants given in Table II. The intermediate dashed curves only serve to join data of equal "age" and to not represent any theoretical model.

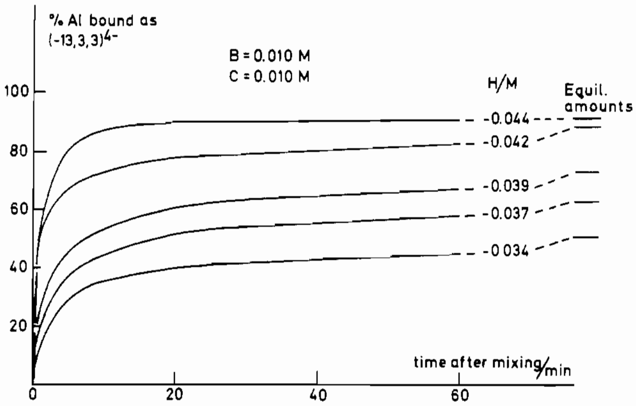

Figure 2. Percentage of Al(III) bound in $(-13,3,3)^{4-}$ as a function of the time after solution preparation.

Data, Calculations, and Results

Kinetic Effects in Slightly Acidic Solutions. Preceding the start of data collection, a large number of theoretical titration curves at different B and C values and C/B ratios were constructed by using the different published complexation models.[8-13] From these calculations it was concluded that the best area to distinguish between different suggested models was at C/B ratios around 1. At higher ratios, the observable differences were strongly diminished by the ionization of unbound citric acid, while at lower C/B ratios, the hydrolysis of Al^{3+} became extensive.

A series of kinetic experiments, as outlined under Method in the Experimental Section, was therefore conducted at $B = C =$ 0.010 M. The results of these experiments are illustrated in Figure 1. From this figure, it can first of all be concluded that the model presented in Table I (solid line in the figure) gives an excellent explanation of equilibrium data in slightly acidic solutions. The reversal in –log $[H^+]$ drift direction with time when H passes the value –0.0433 M is another very strong piece of evidence for the stoichiometry of the dominating, slow-forming species $(-13,3,3)^{4-}$.

To evaluate the stoichiometry and formation constants of species that initially form in these solutions, the formation constant for (–13,3,3) was put to zero, and a number of LETAGROP calculations were performed on "time zero" data. These "time zero" data were extrapolated from the first 3 min of emf readings. The results of these calculations were that data could be explained by the occurrence of the two mononuclear species $(-4,1,1)^-$ and $(-5,1,1)^{2-}$ with $\log (\beta_{-4,1,1} \pm 3\sigma) = -8.48 \pm 0.13$ and $\log (\beta_{-5,1,1} \pm 3\sigma) = -14.71 \pm 0.14$, respectively; $\sigma(H) = 0.0005$ M. The theoretical curve generated by these constants is indicated by the dotted curve in Figure 1.

---

(15) Öhman, L.-O.; Forsling, W. *Acta Chem. Scand., Ser. A* **1981**, *A35*, 795–802.
(16) Öhman, L.-O.; Sjöberg, S.; Ingri, N. *Acta Chem. Scand., Ser. A* **1983**, *A37*, 561–568.
(17) Baes, C. F.; Mesmer, R. E. *The Hydrolysis of Cations*; Wiley: New York, 1976.
(18) Dyrssen, D. *Vatten* **1984**, *40*, 3–9.
(19) Eriksson, G. *Anal. Chim. Acta* **1979**, *112*, 375–383.
(20) Ingri, N.; Sillén, L. G. *Ark. Kemi* **1964**, *23*, 97–121.
(21) Arnek, R.; Sillén, L.-G.; Wahlberg, O. *Ark. Kemi* **1969**, *31*, 353–363.
(22) Brauner, P.; Sillén, L. G.; Whiteker, R. *Ark. Kemi* **1969**, *31*, 365–376.
(23) Sillén, L. G. *Acta Chem. Scand.* **1962**, *16*, 159–172.
(24) Sillén, L. G.; Warnqvist, B. *Ark. Kemi* **1969**, *31*, 341–351.

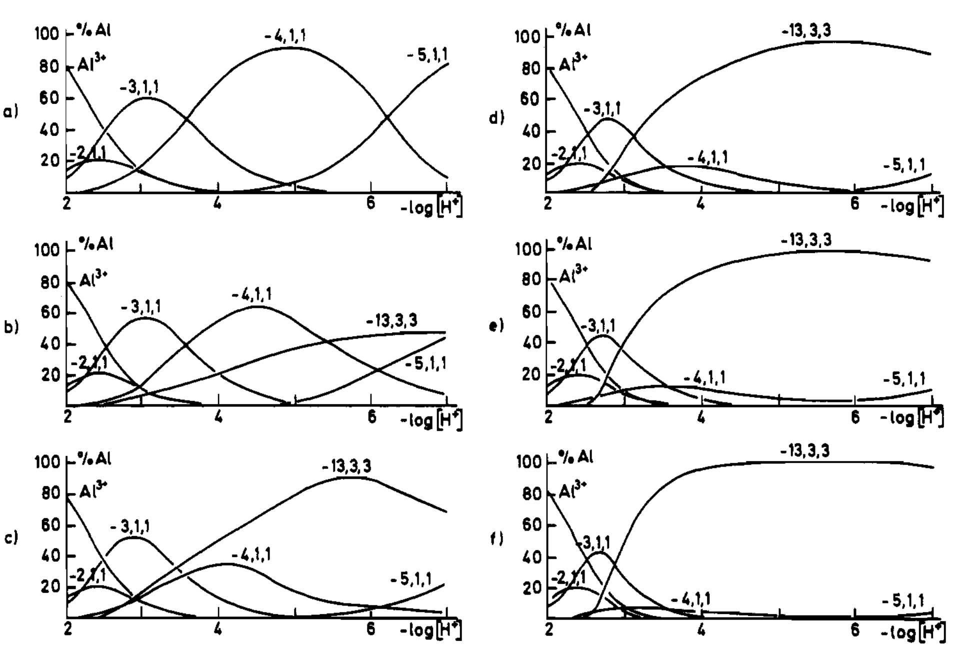

Figure 3. Distribution diagrams showing the amount of different Al-containing species as a function of −log [H$^+$] at different times after mixing ($B = C = 0.010$ M): (a) at mixing time; (b) after 1 min; (c) after 5 min; (d) after 20 min; (e) after 1 h; (f) at equilibrium.

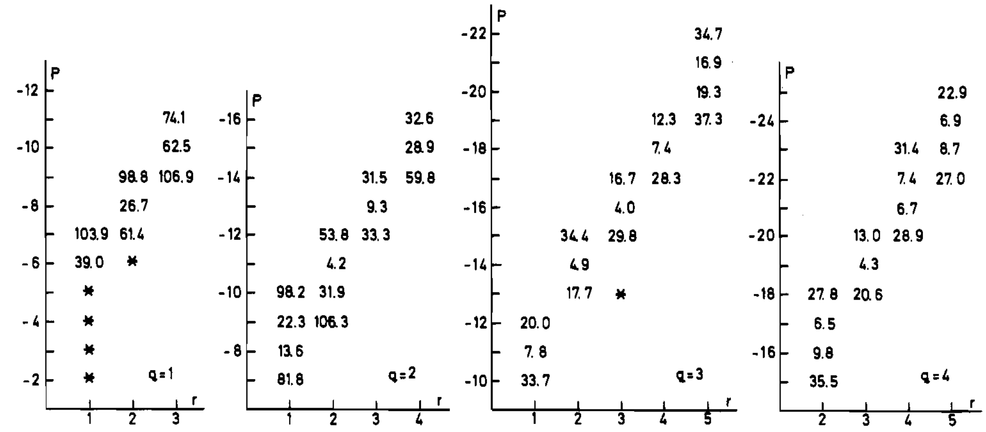

Figure 4. Result of a *pqr* analysis for data with $7 < -\log [H^+] < 9.5$. The figures give the error squares sums $U_H(pr)_q$ with the assumption of one new complex. In the calculations, data from Table I and the complexes $(-4,1,1)^-$ and $(-5,1,1)^{2-}$ have been assumed to be known. The calculations are based on 47 experimental points giving $U_H(00)_0 = 106.9$.

As the solution ages, these complexes are converted into the thermodynamically more stable species $(-13,3,3)^{4-}$. Depending on the amount of hydroxide ions bound in the mononuclear species as compared to the amount of hydroxide ions bound in the trinuclear species, this will result in a net consumption ($H > -43.3$ mM) or release ($H < -43.3$ mM) of hydroxide ions; i.e., the solution −log [H$^+$] will change with time. Thus, the experimentally determined −log [H$^+$] time scales (cf. Figure 1) can be used to evaluate the kinetics by which the species $(-13,3,3)^{4-}$ is formed. The result of this evaluation is given in Figure 2.

On the basis of these data, Figure 3 was constructed. The figures show a gradual increase of the trinuclear species with time at the expense of the initially formed mononuclear species. At equilibrium, only very minor amounts of $(-4,1,1)^-$ and $(-5,1,1)^{2-}$ remain. It can also be seen that the existence area for the uncharged species AlCit^0 is significantly reduced with time.

Equilibria in Slightly Alkaline Solutions. As can be directly spotted in Figure 1, the equilibrium model presented in Table I cannot give a satisfactory explanation for experimentally determined equilibrium data in this region. Evidently, the assumption of a direct transfer from the species $(-13,3,3)^{4-}$ to the aluminate ion, $Al(OH)_4^-$, is incorrect. To evaluate the stoichiometry and stability of the intermediate species, data with the largest variation possible in B, C, C/B, and −log [H$^+$] must be collected. As the kinetic experiments had indicated that equilibria were very sluggish in this region as well, it was decided to perform this data collection in the form of batch experiments. Approximately 60 batches of alkaline aluminum–citrate solutions within the ranges $0.0005 \leq B \leq 0.010$ M, $0.0005 \leq C \leq 0.010$ M, $C/B = 1$, 2, and 4, and $7 < -\log [H^+] < 9.5$ were prepared and stored under an argon atmosphere for 1 week. After that time, turbidimetric measurements were undertaken and all solutions containing precipitates were discarded. On the remaining 47 clear samples, the equilibrium −log [H$^+$] was measured and used in the search for the equilibrium model.

This search was performed as a *pqr* analysis (systematic testing of different p,q,r combinations) with the simple hypothesis that only one additional complex $H_pAl_q(H_3Cit)_r^{p+3q}$ was present. The result of this analysis is given in Figure 4, and it can be seen that a complex of the stoichiometry $(-16,3,3)$ with $\log (\beta_{-16,3,3} \pm 3\sigma) = -47.11 \pm 0.09$, $\sigma(H) = 0.0003$ M, gives the "best fit". It can, however, also be seen that several other polynuclear species give rise to comparable error squares sums. The reason for this becomes obvious when the theoretical curves corresponding to the different species are constructed (Figure 5). Only at $-\log [H^+] \approx 9$ can analytically distinguishable differences be expected. In Figure 6, a magnified version of this region is plotted together with experimental data from two kinetic experiments. From these experiments, it can be concluded that the composition $(-16,3,3)$ obviously is the correct alternative. By the experiment initiated from the H level −0.0433 M, i.e. a solution highly dominated by the species $(-13,3,3)^{4-}$, it is furthermore indicated that the species

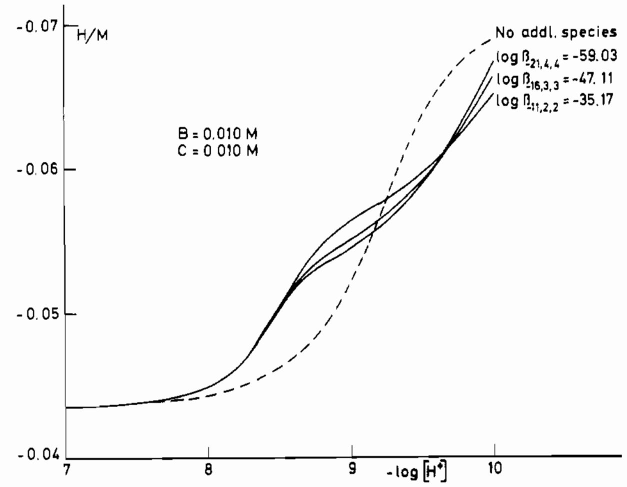

Figure 5. Theoretical H vs $-\log$ [H$^+$] curves, with different polynuclear Al-containing species assumed to be present ($B = C = 0.010$ M).

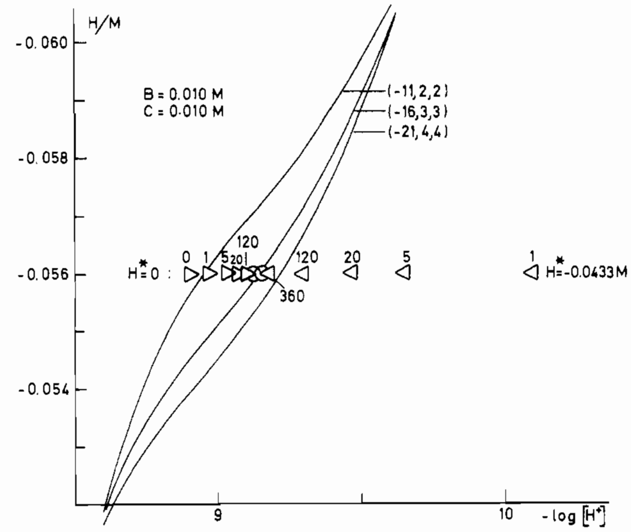

Figure 6. Magnified version of Figure 5 in the part where the different models differ. Results of two kinetic experiments ($B = C = 0.010$ M) with $H^* = 0$ (▷) and $H^* = -0.0433$ M (◁) indicate (a) that $(-16,3,3)^{7-}$ is the correct stoichiometry and (b) that $(-13,3,3)^{4-}$ and $(-16,3,3)^{7-}$ are *not* structurally interrelated.

Table II. Complementary Complexes in the System H$^+$–Al^{3+}–Citric Acid As Determined in the Present Work[a]

(p,q,r)	tentative struct	$\log (\beta_{p,q,r} \pm 3\sigma)$
$(-4,1,1)$	$Al(H_{-1}Cit)^-$	-8.48 ± 0.13
$(-5,1,1)$	$AlOH(H_{-1}Cit)^{2-}$	-14.71 ± 0.14
$(-16,3,3)$	$Al_3(OH)_4(H_{-1}Cit)_3{}^{7-}$–	-47.11 ± 0.09

[a] The formation constants are related to the reaction $p\mathrm{H}^+ + q\mathrm{Al}^{3+} + r\mathrm{H_3Cit} \rightleftarrows \mathrm{H}_p\mathrm{Al}_q(\mathrm{H_3Cit})_r{}^{p+3q}$, and the errors given correspond to $3\sigma(\log \beta_{p,q,r})$.

$(-16,3,3)^{7-}$ is *not* a simple deprotonated form of $(-13,3,3)^{4-}$, as this would have been manifested through a fast attainment of equilibrium in that solution.

As a final model for the complex formation of Al^{3+} with citric acid, it is therefore proposed that, in addition to the complexes given in Table I, species with the (p,q,r) notations $(-4,1,1)^-$, $(-5,1,1)^{2-}$, and $(-16,3,3)^{7-}$, with the equilibrium constants given in Table II, should be included. In order to visualize the amounts of the different species, a number of equilibrium distribution diagrams are presented in Figure 7.

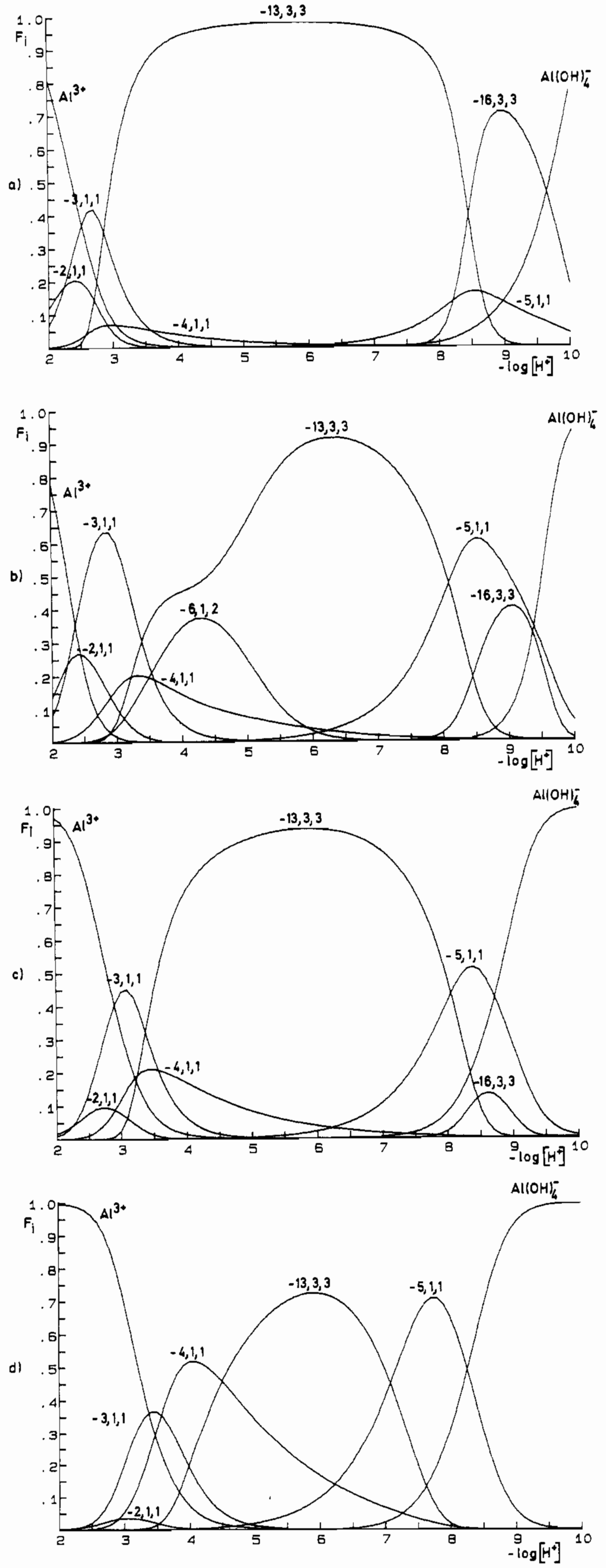

Figure 7. Distribution diagrams of F_i (fraction of total aluminum(III)) versus $-\log$ [H$^+$]: (a) $B = C = 0.010$ M; (b) $B = 0.001$ M, $C = 0.010$ M; (c) $B = C = 0.001$ M; (d) $B = C = 0.0001$ M. The calculations have been performed by using the computer program SOLGASWATER[19] with constants given in the tables.

Discussion

In the present study, equilibrium as well as kinetic potentiometric data[33] have been used to investigate the ability of citric acid to form complexes with the Al^{3+} ion. From the data presented, it can be concluded that this is a system characterized by very slow and complicated equilibrium reactions. Without doubt, this is the reason why published complexation models[8-13] show such divergence.

As illustrated in Figure 3, the species dominating near the time of mixing are quite different from those dominating at true equilibrium. As a consequence, data collected through continuous potentiometric titrations with improper time intervals between base additions will reflect an intermediate behavior. Furthermore, through the continuous collection of these data, with a certain "equilibration" time at each point, the distance from true equilibrium will most certainly vary within the data material. Therefore, the interpretation of such data in terms of complexation models will be highly questionable.

In the present paper, a fresh acidic solution was used to study each level in *H*. With this precaution, it was possible to distinguish between initially formed species and equilibrium species. To describe the intermediate behavior, the simple assumption was made that the mononuclear species $(-4,1,1)^-$ and $(-5,1,1)^{2-}$ were converted into the trinuclear species $(-13,3,3)^{4-}$ without any further intermediate species appearing. Although this of course can be questioned, especially as it results in a pH-dependent time constant for the formation of the trinuclear species (Figures 2 and 3), present indirect data do not permit any more detailed analysis. Probably, a more direct method, for instance time-dependent ^{27}Al NMR spectroscopy, would provide an answer to this question. What present data definitely do show, however, is that unless a slightly acidic aluminum–citrate solution in the millimolar range is only a few seconds old, the appearance of polynuclear species in it cannot be overlooked.

With regard to equilibrium species appearing in slightly alkaline solutions, the present study has given evidence for the formation of another slow-forming trinuclear species, $(-16,3,3)^{7-}$. From Figure 7 it can be concluded that this species is much less stable than the trinuclear species appearing in slightly acidic solutions. Also, the kinetic experiment performed at $B = C = 0.010$ M and $H = -0.056$ M (Figure 6) showed that although the two species have a close (p,q,r) resemblance, they are probably not structurally interrelated.

In ref 11, an attempt to determine the end-point stoichiometry of species appearing in this region with $C/B = 0.0025$ M/0.0002 M was made. The result obtained was that the prevailing complex formed released two protons per aluminum over the Cit^{3-} level. This is quite in agreement with present data, which, under such conditions (Figure 7), implicate a dominance of the species $(-5,1,1)^{2-}$. These authors also observed the slow kinetics connected with the formation of $(-16,3,3)^{7-}$ at higher aluminum concentrations. No attempt was made, however, to determine the stoichiometry and stability of this species.

From Figure 7 it can also be concluded that significant equilibrium amounts of $(-5,1,1)^{2-}$, $(-16,3,3)^{7-}$, and $Al(OH)_4^-$ simultaneously appear in slightly alkaline solutions. In an attempt to validate the appearance of $(-5,1,1)^{2-}$ also from equilibrium data, a calculation was performed on the set of alkaline data, in which the stability constants for all these species were co-varied. The result of this calculation ($\log \beta_{-5,1,1} = -14.83 \pm 0.22$, $\log \beta_{-16,3,3} = -47.12 \pm 0.10$, $\log \beta_{-4,1,0} = -23.34 \pm 0.09$, $U = 2.4$) gives full support for the formation of $(-5,1,1)^{2-}$. In this calculation, the formation constant for $Al(OH)_4^-$ became somewhat higher than reported earlier.[16] This change does not, however, significantly affect the distribution diagrams given in Figure 7.

With respect to the structures of the different species formed, an investigation of this kind gives no direct information. On the basis of the ^{13}C NMR data and stability constant comparisons presented in ref 8, it does, however, seem plausible that the uncharged species $(-3,1,1)$ is a complex where the citrate ion serves as a tridentate ligand with the two terminal carboxylate groups and the deprotonated hydroxy group being coordinated to the Al^{3+} ion, leaving the central carboxylic acid group protonated and unbound.

Accordingly, it seems plausible that the species $(-4,1,1)^-$ is a complex where this carboxylic acid group has been deprotonated. This assumption is also supported by the fact that the pK_a value for $(-3,1,1)$, 3.6, closely resembles the value found for the microconstant of the central carboxylic acid group of unbound citric acid, pK_a = 3.4.[25]

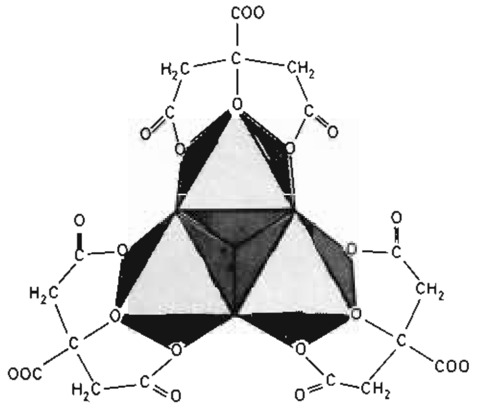

Figure 8. Tentative structure for the species $(-16,3,3)^{7-}$ based on an assumed resemblance with pure Al hydrolysis.

Finally, the last mononuclear species in the series, $(-5,1,1)^{2-}$, without doubt is a mixed hydroxo species, as the maximum number of ionizable protons in citric acid is exceeded. It can probably be described as a hydrolysis product of the complex $Al(H_{-1}Cit)^-$, i.e. $Al(OH)(H_{-1}Cit)^{2-}$, with a pK_a value of 6.2. This value is lower than acidity constants earlier found for AlL_2^- species in the systems H^+–Al^{3+}–salicylic acid[26] (7.60) H^+–Al^+–pyrocatechol[27] (8.01), and H^+–Al^+–1,2-dihydroxynaphthalene-4-sulfonate[16] (8.04). A probable cause of this increased acidity is the higher electron demand within carboxylate groups compared to that within phenolic oxygen groups.

With respect to the two slow-forming trinuclear species, experimental data indicate that the structures of these species are quite different. With regard to the more acidic species, $(-13,3,3)^{4-}$, a possible structure based on the finding that a citrate ion bridges three metal ions in magnesium citrate decahydrate[28] was made in ref 9. Following the publication of that paper, extensive attempts were made to prepare a single crystal of the complex. Unfortunately, however, it turned out that this complex is extremely water-soluble and that, in a solution prepared from $AlCl_3\cdot 6H_2O$, Na_3Cit, and NaOH with Al/Cit/OH = 1:1:1.33, sodium chloride was the most insoluble compound. Even when the solution was evaporated to syrup consistency, only NaCl precipitated. An ^{27}Al NMR spectrum of a 1/1 molar solution of this composition gave one broad peak ($\nu_{1/2}$ = 1600 Hz) at δ = 12 ppm vs $Al(H_2O)_6^{3+}$, thereby indicating that the aluminum ions in the complex are octahedrally coordinated.

Thus, it is still impossible to suggest any conclusive structure for this complex. However, in view of the strong deprotonation tendency predicted for the hydroxy group in the series of monomeric species, this complex should probably be written $Al_3(OH)(H_{-1}Cit)_3(H_2O)_5^{4-}$ rather than $Al_3(OH)_4(Cit)_3(H_2O)_2^{4-}$.

The more alkaline trinuclear species $(-16,3,3)^{7-}$ is formed in a pH range where the dominating species in a freshly prepared solution is $Al(OH)(H_{-1}Cit)^{2-}$. It is therefore tempting to assume that this trinuclear species is a polymerization product of the monomer.

In the pure Al hydrolysis, it has earlier been shown[15,29] that considerable amounts of $AlOH^{2+}$ polymerize to $Al_3(OH)_4^{5+}$. In analogy with that, a reasonable formula for $(-16,3,3)^{7-}$ is $Al_3(OH)_4(H_{-1}Cit)_3^{7-}$ with a structure as given in Figure 8.

Modeling on Natural Systems. In earlier parts of this series, the potential abilities of various ligands to affect the aquatic behavior of aluminum in natural water systems have been indicated via computerized solubility modeling of the clay mineral kaolinite as a function of pH and total ligand concentration. Thus, in ref 9, it was concluded that the presence of citrate ions could be

---

(25) Martin, R. B. *J. Phys. Chem.* **1961**, *65*, 2053–2055.
(26) Öhman, L.-O.; Sjöberg, S. *Acta Chem. Scand., Ser. A* **1983**, *A37*, 875–880.
(27) Öhman, L.-O.; Sjöberg, S. *Polyhedron* **1983**, *2*(12), 1329–1335.
(28) Johnson, C. K. *Acta Crystallogr.* **1965**, *18*, 1004–1018.
(29) Hedlund, T.; Sjöberg, S.; Öhman, L.-O. *Acta Chem. Scand., Ser. A* **1987**, *A41*, 197–207.

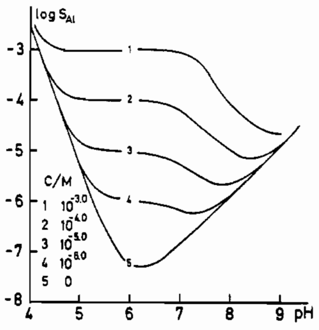

Figure 9. Solubility of gibbsite expressed as log S_{Al} versus pH for different total concentrations of citric acid, *C*.

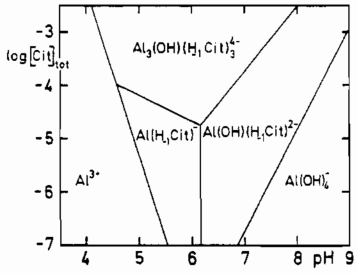

Figure 10. Predominance area diagram showing dominating aqueous Al species in equilibrium with gibbsite as function of log *C* and pH.

expected to cause an extensive solubilization of kaolinite in slightly acidic solutions, mainly due to the formation of the species $Al_3(OH)(H_{-1}Cit)_3(H_2O)_5^{4-}$. As polynuclear species in general are disfavored in dilute solutions, the present inclusion of two additional mononuclear species, $Al(H_{-1}Cit)^-$ and $Al(OH)(H_{-1}Cit)^{2-}$, can be expected to enhance this predicted solubilization, especially at low citrate concentration. Furthermore, the inclusion of two "alkaline" species, $Al(OH)(H_{-1}Cit)^-$ and $Al_3(OH)_4(H_{-1}Cit)_3^{7-}$, can be expected to extend the solubilization effect of citrate ions to higher pH values.

Both of these expectations are validated in Figure 9, a figure that shows the equilibrium solubility of crystalline gibbsite (log $^*K_{s0} = 9.6$) versus pH for various total concentrations of citric acid. The importance of the two added mononuclear complexes are clearly demonstrated in the corresponding predominance area diagram given in Figure 10.

When the solubility-limiting phase is changed from kaolinite to aluminum hydroxide in these calculations, the influence of the degree of crystallinity in the solid phase can also easily be indicated. Thus, in ref 30, a value of log $^*K_{s0} = 11.2$ was determined for a freshly precipitated, amorphous aluminum hydroxide phase. When this solubility product is applied to the solid phase, the solubility and predominance area diagrams have the appearances given in parts a and b, respectively, of Figure 11. As can be seen, the solubility curves are all shifted upward and the solubility drops in slightly alkaline solutions more or less vanish. In the predominance area diagram, the increased concentrations of Al^{3+} and hydrolytic species cause the predominance areas of citrate complexes to decrease.

In the blood plasma of man, citrate ions are present to an extent of 10^{-4} M.[31] To model the behavior of aluminum in such a solution, it is, however, unrealistic to assume that the total aluminum concentration is regulated by a solid phase. A more realistic simulation in this case is to calculate, as is done in ref 31 and 32, the distribution of different species as a function of pH at a total Al concentration of 10^{-6} M, a value typically found in blood plasma. The result of this calculation is shown in Figure 12. From this figure it can be concluded that the dominating species under physiological conditions is $Al(OH)(H_{-1}Cit)^{2-}$. It can also be concluded that the appearance of polynuclear species in blood plasma is negligible, not only from a kinetic point of view but also from a thermodynamic point of view.

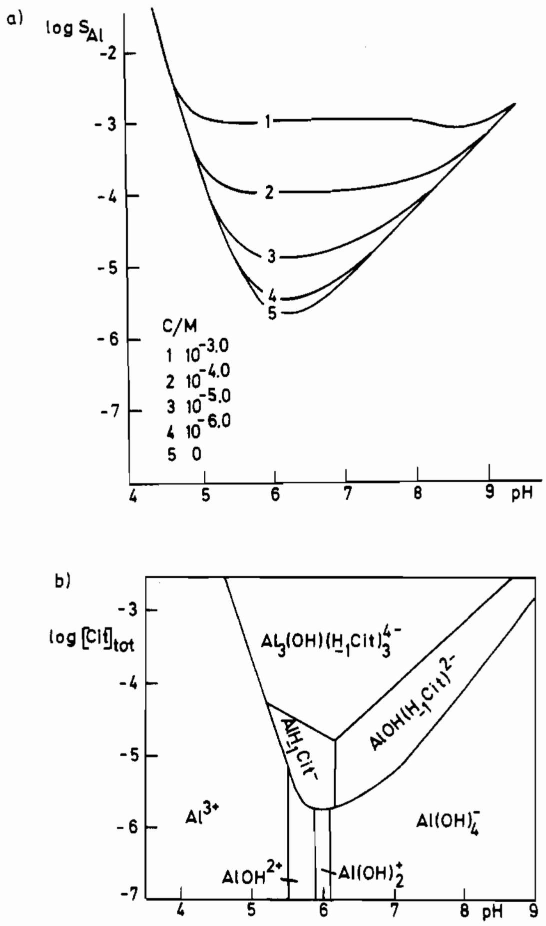

Figure 11. Solubility (a) and predominance area (b) diagrams assuming a solubility regulated by a highly amorphous aluminum hydroxide phase.

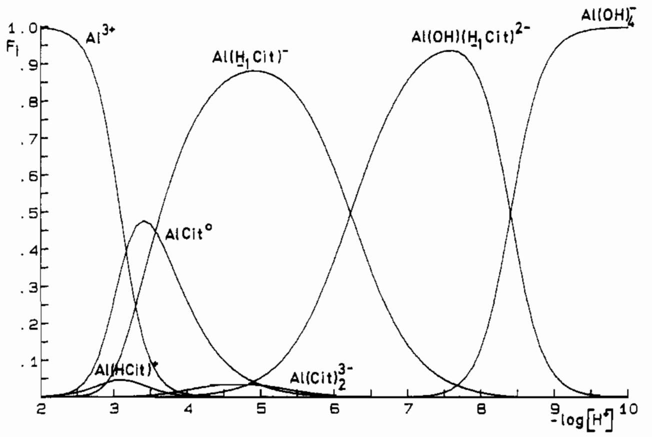

Figure 12. Distribution diagram of F_i versus $-\log [H^+]$ for $B = 1 \times 10^{-6}$ M and $C = 1 \times 10^{-4}$ M.

Acknowledgment. I gratefully acknowledge Professor Staffan Sjöberg for constructive discussions and valuable comments on the manuscript. This work is part of a program financially supported by the Swedish Natural Science Research Council.

---

(30) Öhman, L.-O.; Sjöberg, S. *Mar. Chem.* **1985**, *17*, 91–97.
(31) Martin, R. B. *J. Inorg. Biochem.* **1986**, *28*, 181–187.
(32) Martin, R. B. *Clin. Chem. (Winston-Salem, N.C.)* **1986**, *32*, 1797–1806.
(33) A complete list of the experimental data is available from this department.